Key Regulatory Pathways, MicroRNAs, and Target Genes Participate in Adventitious Root Formation of Acer Rubrum L

Wenpeng Zhu
Beijing University of Agriculture
Manyu Zhang
Beijing University of Agriculture
Jianyi Li
Beijing University of Agriculture
Hewen Zhao
Beijing University of Agriculture
Kezhong Zhang (zhangkezhongbua@163.com)
Beijing University of Agriculture
Wei Ge
Beijing University of Agriculture

Research Article

Keywords: Acer rubrum L1, adventitious roots2, Phylogeny3, Auxin response factors4, Ar-miR160a5

Posted Date: November 9th, 2021

DOI: https://doi.org/10.21203/rs.3.rs-793059/v2

Abstract

Background

Acer rubrum L. is a colorful ornamental tree with great economic value. Because this tree is difficult to root under natural conditions and the seedling survival rate is low, vegetative propagation methods are often used. Because the formation of adventitious roots (ARs) is essential for the survival of asexual propagation of *A. rubrum*, it is necessary to investigate the molecular regulatory mechanisms in the formation of ARs of *A. ruburm*. To address this knowledge gap, we sequenced the transcriptome and sRNA of the *A. rubrum* variety 'Autumn Fantasy' using high-throughput sequencing and explored changes in gene and microRNA (miRNA) expression in response to exogenous auxin treatment.

Results

We identified 82,468 differentially expressed genes between the treated and untreated ARs, as well as 48 known and 95 novel miRNAs. We also identified 172 target genes of the known miRNAs using degradome sequencing. Two regulatory pathways (ubiquitin mediated proteolysis and plant hormone signal transduction), Ar-miR160a and the target gene *ArARF10* were shown to be involved in the auxin response. We further investigated the expression patterns and regulatory roles of *ArARF10* through subcellular localization, transcriptional activation, plant transformation, qRT-PCR analysis, and GUS staining.

Conclusions

Differential expression patterns indicated the Ar-miR160a-*ArARF10* interaction might play a significant role in the regulation of AR formation in *A. rubrum*. Our study provided new insights into mechanisms underlying the regulation of AR formation in *A. rubrum*.

Background

Red maple (*Acer rubrum* L.), a large deciduous tree in family Aceraceae Juss [1], is often used to beautify urban gardens due to its strong adaptability and rapid growth [2]. However, this tree struggle to root under natural conditions, and the survival rate of naturally rooted seedlings is low [3]. Therefore, some red maple varieties, such as the *A. rubrum* hybrid 'Autumn Fantasy', are primarily vegetative propagated using softwood cuttings [1,4].

Adventitious root (AR) formation is a critical aspect of cultivation for most forest species that are vegetative propagated from elite genotypes [5]. AR formation is a developmental process wherein new roots are generated spontaneously (or in response to certain stimuli) from stems, leaves, or the non-pericycle tissues of older roots [6]. In particular, AR formation provided the basis for clonal multiplication, a technique that was utilized for the breeding and propagation of many crop and forestry plants [7]. Auxin, which is formed in roots and stems, and which is involved in stem cell maintenance and differentiation, effectively induce AR formation [8,9]. Auxin dosage, gradient, and response are all important for plant root

growth[10]. Synthetic auxins, such as indole-3-butyric acid (IBA), have been used to induce AR for almost 80 years [11,12]. However, the molecular mechanisms regulating hormone-induced AR development in forest tree species remain incompletely understood.

Although molecular studies have identified several genes associated with AR in model plant species, such as *Arabidopsis thaliana* and *Populus* [6,13], only a few genes that regulated AR have been identified in horticultural plants[14], and most of these encoded transcription factors (TFs)[14]. In total, 35 genes encoding transcription factors were shown to exhibit significant changes in expression level during AR growth and development in *Populus*[15]. However, the functions of most of these genes remain unknown.

By contrast, several genes and proteins associated with AR have been characterized in *A. thaliana*[16]. In particular, auxin response factors (ARF) are the transcription factors that regulate the expression of auxin response genes[17]. Studies of *A. thaliana* and *Populus* ARF mutants have shown that ARFs play important roles in plant growth and development. For example, in *A. thaliana*, single mutations in *ARF7* or *ARF19* reduced the numbers of both lateral and adventitious roots, and the numbers of lateral and adventitious roots were even more drastically reduced in *ARF7/ARF19* double mutants[18]. Compared with wildtype (WT) poplars, transgenic poplars overexpressing *ARF17.1* (*Pro35s::PeARF17.1*) had numerous stems, no obvious trunk, and an increased number of ARs[19]. ARFs were strongly inhibited by members of the equally large Aux/Indole-3-Acetic Acid (Aux/IAA) protein family (29 members in *A. thaliana*) and its core inhibitor TOPLESS [20]. Key to the regulation of auxin signaling is the ubiquitin-26S proteasome system [21] - dependent disassembly of Aux/IAA proteins by a four-member family of SCF E3 ligases assembled with transport inhibitory response 1 (TIR1) F-box proteins or its relatives AuxinBinding F-Box 1 (AFB1), AFB2, and AFB3 [21].

AR development is also regulated by microRNAs (miRNAs), including miR160, miR167, and miR396[16]. miR160, in conjunction with auxin, was shown to regulate the gene expression of *ARF10*, *ARF16,* and *ARF17*; plants overexpressing miR160c produced shorter roots[22]. miR167-*IAA-Ala Resistant3 (IAR3*) influenced lateral root development[23,24]. In cherry radish, the upregulation of miR160-*ARF16*, in conjunction with lengthier photoperiods, was shown to drive rapid root formation [25]. Using high-throughput sequencing, it was shown that the target genes of miR160 and miR390 were related to auxin signaling and involved in the formation of apple rootstock[26]. Finally, miR396 regulated the transition of root stem cells into transit-amplifying cells by interacting with growth-regulating factor (GRF) in *A. thaliana* [27]. miRNAs may also influence AR growth by targeting ARFs [17]. For example, in *A. thaliana*, miR160a, miR160b, and miR160c, which had the same mature sequence, target *ARF10*, *ARF16,* and *ARF17*, respectively [22]. By targeting ARFs, the miR160 family affected the auxin signaling pathway, and thus played an important regulatory role in root growth and development [16].

Despite these previous studies in model plans such as *A. thaliana* and poplar, the AR-associated functions of many miRNAs remain unknown in most horticultural tree species. To address this knowledge gap, we aimed to systematically identify candidate miRNAs that may be involved in AR development in *A.*

rubrum. In addition, to investigate the AR-associated regulatory miRNA network, we aimed to characterize the expression profiles of miRNAs and their targets during *A. rubrum* root development. To this end, we constructed RNA-seq, sRNA-seq, and degradome libraries from the ARs of *A. rubrum* 'Autumn Fantasy'. We then used bioinformatics approaches to identify AR-associated regulatory pathways, to identify transcription factors and miRNAs associated with those regulatory pathways, and to characterize the expression profiles of the identified miRNAs and their targets. Finally, to further explore the regulation of *ArARF10* by Ar-miR160, we overexpressed Ar-miR160 in *A. thaliana* and assessed produced root numbers and lengths.

Methods

The use of plant materials and ethical approval statement

This study including sample collection was conducted according to China's Biodiversity Conservation Strategy and Action Plan (2011–2030) (Index number: 000014672/2010–00714) and Seed Law of the People's Republic of China (2015 Revised Version), which permits use of biological resources to Chinese for scientific research purpose.

Plant materials

We collected full and semi-woody annual branches (60 cm in length) from *A. rubrum* hybrid 'Autumn Fantasy' trees, and the branches were made into 8-10 cm cuttings with two nodes. Cuttings were disinfected with 0.5% potassium permanganate solution, and then soaked in 100 mg/L, 200 mg/L, 300 mg/L, 400 mg/L, or 500 mg/L IBA for 1 h to induce AR formation (n = 50 branches per group). The depth of the cuttings is 3cm. Control cuttings were soaked in clean water for one hour (n = 50). Cuttings were then grown in a greenhouse under a 16 h light (25ºC)/8 h dark (18°C) photoperiod. After 30 days of growth, roots were washed and the numbers of ARs were recorded. The ARs from branches soaked in 300 mg/L IBA and in clear water were stored at -80°C for RNA sequencing (RNA-seq), small RNA sequencing (sRNA-seq), and degradome sequencing.

RNA isolation, library construction, and sequencing

Total RNAs were respectively isolated from CK and IBA300 group using a Trizol Reagent (Invitrogen, Carlsbad, CA, USA) according to the published protocols. RNA samples were checked by Nanodrop 2000 (Thermo Fisher Scientific, Waltham, MA, USA). After checking the RNA quality, the mRNA was reverse transcribed by PrimeScriptTM (Takara, China). Finally, double-stranded cDNA was purified using a DNA purification kit (QIAGEN, Germany) to generate high quality cDNA. Libraries were prepared from a 300-500 bp size-selected fraction following adapter ligation and agarose gel separation. The libraries were sequenced using a paired-end read protocol with 100 bp of data collected per run on the Illumina Hiseq 2000.

The sRNA libraries were constructed using a NEBNext® Multiplex Small RNA Library Prep Set for Illumina®. Finally, the sRNA libraries were sequenced on a BGISEQ-500 system.

mRNA was captured by magnetic beads. Mixed biotinylated random primers and mRNA were used for reverse transcription. After the whole library preparation was completed, the constructed library was sequenced by Illumina hiseq2500, with a single-ended read length of 1×50bp.

Bioinformatics analysis of the sequencing data

For the Transcriptome sequencing data, raw data were filtered by removing adapters and low quality data. The clean data were assembled using Trinity version 2.0.6 [72]. The transcripts were clustered and de-redundant using Tgicl to obtain Unigene [73]. Quality assessment of assembled transcripts was made by comparison with conserved genes using the single-copy direct homology database BUSCO [74]. Potential duplicate molecules were removed from the aligned BAM format records. FPKM (fragments per kilobase of exon per million fragments mapped) values were used to analyze gene expression by the software Cufflinks [75]. New genes were identified based on new discovered transcripts through Cufflinks. The genes encoding peptides with less than 50 amino acid residues were filtered. Differentially expressed genes were detected using DEGseq. Differentially expressed gene (DEGs) were selected with a difference of two-fold or more and the Q-value ≤ 0.001 [76].

For the sRNA sequencing data, raw data were filtered by removing adapters and low-quality data to generate clean reads. Unique sRNAs were aligned to the miRNA precursors of corresponding species in miRBase to obtain a miRNA count. Based on the ability of miRNA precursors to form hairpin secondary structures, we used miRA for novel miRNA prediction using default plant parameters [77]. miRNA expression level was calculated by using Transcripts Per Kilobase Million (TPM) [78], and calculated the fold change and p-value. DEGseq was employed to evaluate differentially expressed miRNAs between IBA300 and CK [76], The P-values calculated for each gene were adjusted to Q-values for multiple testing corrections by two alternative strategies [79]. Differentially expressed miRNAs were selected with fold change ≥2 and Q-value ≤ 0.001.

The standard sequences valuable for the degradome sequences were compared in the database at NRPM (reads per million) to remove redundancy. The Needle program in the EMBOSS package was applied to derive all sequences that matched the sequences in the previous sRNA library, and then the columns were scored according to the plant miRNA/target pairing criteria [80,81]. The mRNA sequences of target genes paired with the sRNA sequences of *A. rubrum* were predicted by Targetfinder, and prediction score cutoff value was selected for four. The target genes corresponding to the predicted miRNAs and the mRNAs in the degradome were combined and operated to find out the common mRNAs which were the target genes of the miRNAs. And the peak classification and score of the degradome are given, and the generated prediction results are plotted [82]. The MFE values for these precursors were predicted using the classic algorithm of Zuker and Stiegler [83].

GO and KEGG enrichment of the differentially expressed genes (DEGs)

Sequence alignment of DEGs with NR, Swiss-Prot, GO, KEGG databases using BLAST software was conducted to obtain annotation information for the DEGs in RNA-seq. We investigated the GO enrichment of DEGs using the Gene Ontology Consortium (http://geneontology.org/); p-values were FDR corrected using DEGseq [76], and terms with Q-value≤0.05 were considered to be significantly enriched in the DEGs. We identified KEGG pathways significantly associated with the DEGs according to expression abundance. Hierarchical clustering of expressional data was carried out using the TBtools [84].

Identification and classification of ARF genes

The twenty-three protein sequences from *A. thaliana* (https://www.arabidopsis.org/) were selected to search against the transcript of *A.rubrum* using Tblastn method. Matrix was BLOSUM62; expect was less than 1e-005; gap-existence was 11; gap-existension was 1; filter was low-complexity. All publicly known *ARFs* of *A.thaliana*、*Citrus sinensis, Dimocarpus longan* were identified based on a BLASTP search at the score value of ≥ 100 and e-value e ≤ e-10 [85,86]. Next, the Pfam database (http://pfam.xfam.org/) was used to determine whether each candidate ARF sequence belonged to the ARF gene family [87]. To exclude overlapping genes, all candidate ARF genes were aligned with ClustalW and checked manually. SMART (http://smart.embl-heidelberg.de/) and InterProScan (http://www.ebi.ac.uk/Tools/pfa/iprscan/) web servers were used to examine the conserved domains of the identified *A.rubrum* genes. Obtained *ArARF* genes were named according to their *A.thaliana* homologs. The protein characteristics, including molecular weight (MW), isoelectric points (pIs) and lengths were online predicted by ProtParam tool.

Phylogenetic and conserved motif analysis of the ArARFs

To explore inter- and intraspecific phylogenetic relationships among ARF proteins, we constructed a dataset of ARF proteins including the ArARFs identified in this study, as well as *ARFs* from 22 *A.thaliana* ARFs, 16 *Dimocarpus longan* ARFs, 18 citrus ARFs (referred as to *AtARF*, *DiARF*, *CsARF* respectively). Neighbor-joining (NJ) phylogenetic analysis of the 74 ARF protein sequences was performed using MEGA7 [76], with 1000 bootstrap (BS) replicates. The best-fit model of nucleotide substitution (i.e., that with the lowest BIC score) was JTT+G+I. All positions with less than 80% site coverage were eliminated; that was, fewer than 20% alignment gaps, missing data, and ambiguous bases were allowed at any position [88,89]. To investigate the structural differences among *ArARF* genes, conserved motifs in the predicted ARF proteins were investigated using online MEME analysis (http://meme.nbcr.net/meme/), with an optimum motif width of 6-50. The maximum number of motifs was set to 10 [90]. Results were visualized using TBtools [91].

Quantitative reverse-transcription PCR (qRT-PCR) assay

qRT-PCRs were performed using a CFX Connect TM Real-Time System. Each total RNA sample (2 μg) was digested with RNase-free DNase I (Invitrogen) to remove genomic DNA contamination and subsequently

reverse transcribed into cDNA using an Oligo (dT)18 primer. For the qRT-PCR of the miRNAs, U6 snRNA was used as the internal control. For the qRT-PCR analyses of the miRNA target genes [92], *Actin6* was used as the internal control [93]. PCR volumes (20 μl) contained 1 μl of 20×diluted cDNA, 5×SYBR buffer, and 0.25 μM forward and reverse primers; the gene-specific primers used for qRT-PCR were given in Table S3. The thermal cycling conditions were as follows: 95°C for 30 s, followed by 40 cycles of 5 s at 95°C and 30 s at 60°C. All reactions were performed in triplicate in three independent experiments. The relative fold-changes in miRNA and gene expression levels were calculated using the $2^{-\Delta\Delta Ct}$ method while *ArARF10* was calculated using the $2^{-\Delta Ct}$ method [94].

Subcellular localization and transcriptional activation

The full-length cDNA sequences of the target gene *ArARF10* were cloned from the cDNA of ARs in *A. rubrum*. The subcellular location of ArARF10 was determined by transfecting GFP-tagged ArARF10 into 3–4-week-old *Nicotiana benthamiana* seedlings. The full-length cDNA of *ArARF10* was fused in-frame with GFP cDNA and ligated between the CaMV 35S promoter and the nopaline synthase terminator. The fluorescence signals in the transfected leaf cells were examined under a confocal laser scanning microscope (Axio Lab A1) [95]. The transcriptional activation of ArARF10 was investigated by transforming the pGBKT7 construct (in which ArAFR10 was fused with the GAL4 DNA-binding domain) into yeast strain AH109. Yeast strain AH109 contains the His-3 reporter genes. The transformants were streaked on the SD/Trp- and SD/Trp-/His- medium. After incubated at 28°C for 3 days, the growth status of the transformants was evaluated. The transformed yeast cells were grown on synthetic defined (SD) media (with or without His); yeast with active His-3 reporter genes were able to grow on synthetic defective plates.

Constructs and plant transformation

We next tested whether the overexpression of Ar-miR160a and *ArARF10* affected the growth and development of *A. thaliana.* The Ar-miR160a-5p precursor was cloned from *A. rubrum* genomic DNA. The precursor sequence of Ar-miR160a-5p and the ORFs of *ArARF10* were cloned into the entry vector pTOPO-T. After verification by sequencing, the fragments of the Ar-miR160a-5p precursor and *ArARF10* inserted into the entry vector were transferred to the destination vector pCAMBIA1301 via an LR reaction. The constructed vectors (*Pro35S::Ar-MIR160a* and *Pro35S::ArARF10*) were driven by the CaMV 35S promoter. The pCAMBIA1301 vector contained a GUS reporter gene initiated by the 35S promoter.

The constructs (*Pro35S::Ar-MIR160a* and *Pro35S::ArARF10*) were introduced into WT *A. thaliana* (Columbia-0) using electroporation and *Agrobacterium*-mediated transformation. Seeds of the plants exhibiting transgenic phenotypes were sterilized and sown on 1/2 Murashige and Skoog (1/2 MS) medium, as described previously [96]. Plates were incubated at 4ºC for 48 h for stratification and then exposed to light for several hours to induce germination. Plates were next wrapped in three layers of aluminum foil and placed in the dark until the seedlings had an average hypocotyl length of 6 mm (48 h). The *A. thaliana* primordium was excised using a sterile blade, preserving about 6 mm of the hypocotyl,

and then the seedlings were exposed to a natural photoperiod (16 h light/8 h dark) to induce AR formation. AR lengths and numbers were measured using ImageJ [97] eight days after transferring to light conditions. For each biological replicate, at least 10 seedlings were analyzed, and each experiment was repeated at least three times. One-way ANOVA, combined with Tukey's multiple comparison tests, were performed using GraphPad Prism 8 to analyze differences in means and variances among genotypes.

GUS staining

After eight days of cultivation, transgenic and WT *A.thaliana* seedlings were washed and completely immersed in GUS staining solution (Coolaber, China). After overnight staining at 37°C in the dark, seedlings were decolorized in 70% ethanol, examined, and photographed.

Availability of data and materials

The sequencing data were submitted to the SRA database with the accession numbers SRR13808891, SRR13808890, SRR13808889, SRR13808888, SRR13808887, SRR13808886, SRR13808885 and SRR13808884.The data that support the conclusions are within this article and its additional files. All data and plant materials used in current study are available from the corresponding author on reasonable request.

Results

Transcriptome, sRNA, and degradome sequencing

After 30 days of growth, all IBA-treated groups (100–500 mg/L IBA) had developed ARs, while only a small amount of AR development was observed in the control group (**Fig. 1**). Importantly, substantially more ARs were developed by the cuttings treated with 300 mg/L IBA; the ARs of these cuttings were also of more consistent length and more densely packed than those formed on the cuttings treated with other concentrations of IBA (**Fig. 1**). Cuttings treated with 300 mg/L IBA treatment had significantly more roots than any other cuttings. Therefore, the ARs from the cuttings treated with 300 mg/L IBA (henceforth referred to as IBA300), as well as those formed by the control cuttings, were selected for transcriptome profiling.

Raw data generated by Illumina HiSeq sequencing were: 200.4 million raw reads from the control samples and 213.29 million raw reads from the IBA300 samples. After quality filtration, 55.48 G of clean data (Q30≥93.69%) remained. The percent of GC content was greater than 38.16%, the AT and GC ratios were within a reasonable range, and there was no separation. We identified 82,468 DEGs (fold-change≥2, FDR<0.01) between the control and IBA300. Of these, 69,777 were upregulated and 12,691 were downregulated. Across all DEGs, 31,385 CDS were detected, and 1,417 Unigene-encoding transcription factors were predicted. The sequencing data were submitted to the SRA database with the accession numbers SRR13808891, SRR13808890, SRR13808889 and SRR13808888.

In total, approximate 51.22-52.42 million high-quality clean reads from the control and IBA300 groups were obtained using sRNA-seq. Most of the sRNAs were 21–24 nt long, with 24 nt sequences being the most common across all samples **(Fig. S1)**. The reads remaining after the removal of tRNAs, rRNAs, snRNAs, snoRNAs, and degraded mRNAs were considered endogenous sRNAs and used in subsequent analyses. The sequencing data were submitted to the SRA database with the accession numbers SRR13808887, SRR13808886, SRR13808885 and SRR13808884.

Analysis of sRNA-seq data showed that 48 known (**Table S1**) and 95 novel miRNAs were identified. The length of mature miRNA varies from 20 to 30nt. Due to the recognition and cleavage of DCL1 enzyme, the first base at the 5' end of each miRNA was biased to U and resistant to G. Across all datasets, the first nucleotide of the novel miRNA was primarily biased towards U, followed by A **(Fig. S2)**. 1,744 target genes cleaved by known miRNAs and 1,956 miRNA-mRNA pairs were predicted using Targetfinder.

To generate a miRNA-cleaved target library (degradome) from *A. rubrum,* we first identified the mRNA transcripts targeted by miRNAs in the total RNA samples using high-throughput sequencing. We obtained 34,373,253 short reads from the control RNA samples and 28,061,482 short reads from the IBA300 RNA samples, representing the 5’ ends of uncapped, poly-adenylated RNAs. After initial processing, equal numbers of 20 and 21nt sequence reads remained. In total, 47.66% of the unique reads were successfully mapped to the *A. rubrum* transcriptome. We identified 172 mRNAs targeted by the known miRNAs and 243 miRNA-mRNA pairs via CleaveLand (**Table S2**). The sequencing data were submitted to the SRA database with the accession numbers SRR13808883 and SRR13808882. Across the 172 mRNAs targeted by the known miRNAs, most were associated with plant hormone signal transduction. Of these, 80 mRNAs were either transcription factors or related to transcription factors, including growth-regulating factors (GRFs), ARFs, SQUAMOSA promoter-binding protein-like (SPL) proteins, MYBs, and ethylene response factors (AP2/ERF). Consistent with the RNA-seq results, many genes were associated with the plant hormone signal transduction pathway. However, only 8.8% of the target genes were identified by degradome sequencing. This suggested that most of the predicting miRNA target genes were false positives.

The T-Plot of five conserved miRNAs and one predicted novel miRNA was shown in **Fig. 2**. Three of the validated differentially expressed miRNAs (Ar-miR160a-5, Ar-miR171d-1, and Ar-miR156f) had previously been shown to target transcription factors.

Pathways and functions associated with the DEGs in *A. rubrum*

Among all the DEGs, GO analysis indicated that 14,451 DEGs were significantly enriched in 30 GO terms between the control and IBA300 groups (27% cellular component terms, 23% molecular function terms, and 50% biological process terms; **Fig. S3**). In particular, the biological process terms “regulation of biological process”, “biological regulation”, “cellular process”, “metabolic process”, “signaling”, and “response to stimulus”; the cellular component terms “macromolecular complex”, “cell junction”, “nucleoid”, “organelle”, “cell part”, and “membrane part”; and the molecular function terms “binding”,

“catalytic activity”, “transcription regulator activity”, and “signal transducer activity” were overrepresented in the DEGs (**Fig. S3**).

Of the 14,451 DEGs, 9,507 were successfully mapped to the KEGG database (P-value < 0.05). KEGG mapping indicated that 59 terms and 12 metabolic pathways were significantly enriched in these DEGs, with the largest numbers of DEGs associated with the MAPK signaling pathway and the plant hormone signal transduction pathways (**Fig. S4**). The log-normalized FPKM values for the significantly enriched metabolic pathways were used for hierarchical clustering analysis (**Fig. 3)**. The significantly upregulated pathways were ubiquitin mediated proteolysis and hormone signal transduction (**Table S4**).

Many of the DEGs associated with the plant hormone signaling pathway were involved in auxin signaling transduction. For example, numerous genes in the families associated with auxin signaling (e.g., AUX, IAA, GH3, ARF, and SAUR) were significantly differentially expressed between the control group and the IBA300 group, including *Aux/IAA5* (Unigene3732_All), *SAUR11* (Unigene73966_All), *Aux/IAA4* (Unigene5767_All), and *ARF18-1* (Unigene5190_All). The expression of 24 genes (i.e., the IAAs, GH3s, ARFs, and SAURs) were upregulated in IBA300 as compared to the control (**Fig. 4a**). Our results indicated that 42 DEGs were involved in the ubiquitin-mediated proteolysis pathway (**Fig. 4b**). Some of these DEGs had been shown to be associated with the mediation of Aux/IAA protein ubiquitination, including S phase kinase-associated protein 1 (SKP1) (Unigene7049_All), cullin 1 (CUL1) (Unigene20934_All), and F-box (SCF) E3 (Unigene17129_All), were significantly upregulated. The patterns of upregulation we observed suggested that the plant hormone signaling pathway and the ubiquitin mediated proteolysis pathway jointly regulate *A. rubrum* root development.

We also performed GO and KEGG analyses of the miRNA target genes. We found that the GO term “DNA binding pathway (GO: 0003677)” was significantly enriched in the target genes (p = 0.003258). KEGG pathway analysis also showed that 10 of the targets of the 220 differentially expressed miRNAs that played a significant regulatory role in the plant hormone signaling pathway belonged to three gene families (ARF, SCL and TGA family) (**Fig. S5**).

qRT-PCR validation of the miRNAs and their targets

Nine miRNAs were selected for qRT-PCR validation. All nine miRNAs were significantly downregulated in the IBA300-treated samples as compared to the control (**Fig. S6**), which was consistent with our sequencing data. Thus, these nine miRNAs might play important regulatory roles in *A. rubrum* growth, especially during rooting.

Next, to reveal the expression patterns of miRNA-mRNA pairs associated with plant hormone signal transduction in *A. rubrum* roots, we quantified the expression levels of six miRNAs and six target genes that were verified to interact by degradome sequencing, and where the target gene was also differentially expressed in the hormone transduction pathway. After IBA treatment, these six miRNAs showed inverse expression patters to the corresponding six target genes (**Fig. 5)**. This was consistent with our RNA and degradome sequencing results. Therefore, we speculated that the Ar-miR160-*ArARF10* interaction might

be critical for the regulation of AR development in *A. rubrum*. The primers used in all quantitative RT-PCR experiments were listed in **Table S3**.

Comparative phylogenetic analysis of the ArARF protein family

Putative *ARF* genes in *A. rubrum* were identified in the RNA-seq data using BLAST. After the removal of redundant sequences and alternative splice forms, 18 ARF proteins were identified as potentially encoded by the *ArARF* genes (**Table S5**). In this study, we designated these proteins ArARF1–ArARF10 and ArARF16–ArARF19. Because the ArARF10 and ArARF19 proteins were encoded by more than one homologous gene, we named the encoding genes as *ArARF1–ArARF10*, *ArARF16–ArARF19, ArARF19-2*, and *ArARF19-3* (**Table S5**). The ORFs of the *ArARF* genes varied from 1,836 bp (*ArARF10*) to 3,510 bp (*ArARF19-3*). These genes encoded polypeptides of 612–1,170 amino acids, with predicted molecular masses of 67.17–131.19 kDa and theoretical pIs of 5.30–8.39 (**Table S5**).

Our Neighbor-joining (NJ) phylogenetic tree, which included 18 ArARFs, 22 AtARFs, 16 DiARFs, and 18 CsARFs, suggested that ArARF homologs were more common in *Dimocarpus longan* and *citrus reticulate* than in *A. thaliana* (**Fig. S7A)**. The ARF genes were clustered into three major, well-supported clades (I–Ⅲ; BS>74; **Fig. S7A**). Seven *ArARF* genes fell into clade Ia, four into clade Ib, one into clade IIa, three into clade IIb, and two into class III (**Fig. S7A**, highlighted in red). Alignment of the ARF proteins indicated that most of the ArARF proteins harbored three characteristic regions (**Fig. S7C**). Unsurprisingly, most of the close homologs in our phylogenetic tree shared common motifs. The three domains of ArARF proteins were comprised of a total of eight different motifs: motif 1, 2, and 3 constituted the DNA-binding domains; motif 6, 8, and 9 constituted the ARF domain; and motif 5 and 10 constituted the C-terminal Aux/IAA domains. Motif 1, 2, 3, 6, 8, and 9 were found in all 18 ArARF proteins (**Fig. S7B**).

Construction of three miRNA-mRNA regulatory networks

The minimum free energy (MFE) values for the precursors of our three focal miRNAs (Ar-miR160a-5p, Ar-miR171d-1, and Ar-miR156f) were −87.10 kcal/mol, −72.90 kcal/mol, and −34.70 kcal/mol, respectively. The precursor sequences had typical stem-loop structures (**Fig. S8**). High-throughput degradome sequencing indicated that Ar-miR160a targeted *ArARF10* (CL3897.Contig1_All) and *ArARF18-1* (Unigene5190_All); Ar-miR171d-1 targeted *ArSCL6-1* (Unigene23148_All) and *ArSCL6-2* (CL2444.Contig4_All); and Ar-miR156f targeted *ArAPL-2* (CL2023.Contig1_All) (**Fig. 6**).

Identification of ArARF10

Expression of fluorescent-tagged ArARF10 in *N. benthamiana* seedlings showed that, while the green fluorescent protein (GFP) control was dispersed throughout the cell (**Fig. 7A-C**), GFP-tagged ArARF10 proteins were located in the nucleus (**Fig. 7D-F**), consistent with their putative function as transcription factors. In addition, ArARF10 fused to the GAL4 DNA-binding domain activated the expression of the His-3 reporter gene in yeast **(Fig. S9**), indicating that this gene was a transcriptional activator.

Overexpression of Ar-miR160a and *ArARF10* in *A. thaliana*

Transgenic plants overexpressing *ArARF10* had much more ARs than WT plants (**Fig. 8 A, B, E, F**), while transgenic plants overexpressing Ar-miR160a had fewer roots than WT plants (**Fig. 8A, C-F**). GUS staining indicated that the transgenic *A. thaliana* seedlings successfully overexpressed Ar-miR160a or *ArARF10* **(Fig. S10)**. Consistent with this, Ar-miR160a and *ArARF10* were significantly more upregulated in the transgenic lines than in the WT lines (*A. thaliana* Columbia-0) **(Fig. 8G**). However, none of these genes was significantly differentially expressed in the transgenic plants except *AtGH3.6*, which was significantly upregulated in the transgenic plant overexpressing *ArARF10* as compared to the WT **(Fig. 8H**).

Discussion

Hormones play a crucial role in the development of plant roots, and interactions among hormones affected root location, root type, and the efficiency of root formation [5]. The plant hormone auxin is commonly used to promote vegetative propagation in woody plants that were difficult to root [6,28]. In such plants, the application of exogenous auxin at an appropriate developmental stage could induce AR formation [29,30]. Our results suggested that 300 mg/L IBA most effectively induced rooting in *A. rubrum* cuttings. It was found that the efficiency of AR formation was Gaussian distribution correlated with the concentration of IBA, indicating that, as in many other woody plants, auxin might play an important role in AR formation in *A. rubrum*.

Because exogenous auxin must be absorbed, transported and metabolized in order to induce AR development [31], a better understanding of the signal transduction and molecular regulation mechanisms underlying the effects of auxin on AR development would help to improve the efficiency of exogenous auxin application during the vegetative propagation of cuttings. To further investigate the molecular mechanisms regulating AR formation in *A. rubrum* in response to IBA treatment, we first identified 9,507 genes that were differentially expressed in IBA-treated *A. rubrum* ARs compared to untreated *A. rubrum* ARs. KEGG pathway analysis suggested that these genes were associated with a total of 134 metabolic pathways. In particular, genes in the tryptophan metabolism, anthocyanin biosynthesis, and nitrogen metabolism pathways were generally downregulated in response to IBA treatment.

Because auxin has such a profound effect on plant growth and development, it seemed that certain checks must be in place to prevent excessive responses. Consistent with this, it has been shown that the PIN auxin efflux carrier genes transported excess auxin out of the cell via a feedback regulation loop [32]. Here, genes in the pathway responsible for synthesizing the auxin precursor tryptophan were generally downregulated after exogenous IBA treatment. Thus, we speculated that exogenous auxin might inhibit the synthesis of internal auxin in *A. rubrum*. However, the changes in expression profiles of genes in the plant hormone signal transduction pathway suggested that appropriate exogenous auxin might prolong AR development, improving rooting.

AR development was characterized by high energy requirements [33,34]. A previous transcriptomic study in carnation indicated that sucrolytic enzymatic activity was regulated at the transcript level during adventitious root induction [35]. Consistent with this, we found that 384 of the DEGs were enriched in the

“starch and sucrose metabolism” (ko00500), while several genes associated with the sucrose metabolism, including *α-glucosidase 3* (Unigene42466_All) and *glucoamylase 1* (Unigene10485_All), were significantly upregulated at the transcriptional level. This implied that the energy provided by the sucrose metabolism was crucial for the development of ARs in *A. rubrum*.

The UPS, which comprised 6% of the *A. thaliana* proteome [21], was a large and complex system of degraded proteins that played a prominent role in hormone regulation [36]. Among the multisubunit ubiquitin ligases of the ubiquitin–26S proteasome system (UPS), the SCF group, consisting of the Skp1, CUL1, and SCF E3 subunits [37], was the most numerous and well-characterized [38,39]. The F-box protein was the substrate selection subunit of the SCF-type ubiquitin protein ligase complex [37]. This dimer transfers activated ubiquitin from the ubiquitin-activating enzymes and bound it to the target proteins [39]. Auxin mediated the binding of Aux/IAA to TIR1/AFBs, and then brought the complex to the SCF for ubiquitination and subsequent degradation [40]. Several studies had been shown that auxin promoted the $SCF^{TIR1/AFB}$ degradation of Aux /IAA proteins [41,42]. Here, most of the ubiquitination-associated DEGs were implicated in the ubiquitination and degradation of Aux/IAA by the SKP1-CUL1-SCF complex, mediated by auxin. In particular, genes that mediated the ubiquitination of Aux/IAA proteins, including SKP1 (Unigene7049_All), CUL1 (Unigene20934_All), and SCF E3 F-box (Unigene17129_All), were significantly upregulated in response to exogenous auxin treatment. This result suggested that auxin-mediation ubiquitination and degradation of Aux/IAA might facilitate AR formation in *A. rubrum*.

Members of the *Aux/IAA* family were short-lived nuclear proteins that played a critical role in suppressing the expression of ARF-activated genes [20,43]. Aux/IAA proteins had been known to bind to ARFs and prevent the activation of auxin-responsive genes in the absence of auxin [44]. At high levels of auxin. Aux/IAA proteins could be ubiquitinated by interaction with the TRANSPORT INHIBITOR RESPONSE 1/AUXIN SIGNALING F-BOX (TIR1/AFB) (Unigene20637_All) receptor and subsequently degraded by the 26S proteasome [45,46]. ARFs with the consensus sequence TGTCTC bind specifically to the AUXIN response element (ARE) [47]. Aux/IAA proteins prevented this activation by forming aggregates with ARF, while auxin regulated the expression level of the ARE promoter downstream of the ARF-binding site by triggering the degradation of Aux/IAA [48]. The $SCF^{TIR1/AFB}$-Aux/IAA-ARF signaling system thus allowed for a diversity of auxin responses. Interestingly, our transcriptome sequencing results indicated that this signaling regulatory system in *A. rubrum* ARs was significantly affected by treatment with exogenous auxin. Altering the transcription of genes in the auxin signaling pathway might be a genetic strategy used by *A. rubrum* in response to auxin alterations. Analysis of these genes might help to identify those that played a key role in AR development.

We identified 14 putative *ArARF* genes in the AR transcriptome of *A. rubrum*, most of which contained an amino-terminal DNA binding domain, a middle region that functioned as the activation or repression domain, and a carboxy-terminal dimerization domain. Four of these genes were significantly upregulated in response to IBA treatment: *ArARF5* (CL11296.Contig1_All), *ArARF17* (CL5608.Contig3_All), *ArARF18-1*

(Unigene5190_All), and *ArARF19-1* (CL1642.Contig1_All). The nuclear targeting of ArARF10 protein was consistent with the transcriptional regulatory function and had a transcriptional activation function. Determination of structural domain function implied that ArARF10 promoted AR development in *A.rubrum* by activating downstream auxin-responsive genes. These results indicated that ArARFs might play different roles during AR development in *A.rubrum* cuttings.

Phylogenetic analysis of the ARF proteins from *A. rubrum*, Longan, *Citrus* sp., and *A. thaliana* suggested that ARF proteins fell into three major clades, consistent with previous evolutionary analyses [49-52]. Consistent with this, previous studies had shown that ARF proteins included a highly conserved region of about 100 amino acid residues in the N-terminal region, corresponding to the DNA-binding domains [53]. Motif analysis identified 10 unique motifs across the 18 ArARF proteins [54]. Notably, ArARF8, ArARF10, and ArARF6-2 exhibited a high degree of homology with DiARF8, DiARF1, CsARF6, CsARF8, and CsARF10. In addition to the high degree of domain conservation and homology in ARF proteins among species, numbers of ARF copies were similar between *A. rubrum* and other species in the Sapindales, including Longan, *Citrus* sp [49,55]. This indicated that species in this order might undergo similar whole-genome duplications, and it was speculated that ARF diversification might represent an adaptation to environmental changes [56].

Although ARF transcription factors have been shown to play a critical role in the regulation of root development and auxin correspondence [57], miRNA interactions with transcription factors and other targets might also influence the regulatory networks that controlled the root transcriptome and might play a key role in the eventual translation of mRNAs [58]. Using sRNA sequencing, we identified six differentially expressed miRNAs associated with plant hormone signal transduction. miR171, *SCL6-II*, *SCL6-III*, and *SCL6-IV* were expressed ubiquitously in plants [59,60]. Transgenic plants overexpressing *MIR171c* (*35Spro–MIR171c*) and *scl6-II scl6-III scl6-IV* triple mutant plants exhibited pleiotropic phenotypes [61], including alterations in shoot branching, plant height, chlorophyll accumulation, root development, flower architecture, and leaf shape and pattern. We found Ar-miR171 cleaved *ArSCL* in *A.rubrum.* Its expression was significantly down-regulated after exogenous IBA treatment, suggesting that the expression of miR171/*SCL* might be related to auxin activity in *A.rubrum*. miR171/*SCL* could play an important role in AR development. In *Arabidopsis*, *SPL* was targeted by miR156. *SPL3*, *SPL9* and *SPL10* were involved in suppressing lateral root growth [62]. In addition, both miR156 and *SPLs* were sensitive to auxin signaling [63]. In our work, we found that Ar-miR156 was sensitive to exogenous IBA and targeted *ArSPL*, suggesting that miR156/*SPL* might be involved in AR development of *A.rubrum*.

Ar-miR160a-5p and Ar-miR160b-1 targeted and cleaved *ArARF10* and *ArARF18-1*. Ar-miR160 and its target gene *ArARF10* showed opposite expression patterns during AR formation in the presence of exogenous auxin. Most miRNAs in the miR160 family regulated plant development through the targeted cleavage of ARFs. Transgenic *A. thaliana* and *Medicago truncatula* overexpressing miR160 had shorter roots than their WT counterparts [22,64], and a study in Longan showed that Dlo-miR160 negatively regulated *DiARF10*, *DiARF16*, and *DiARF17* to affect hormone signaling and somatic embryogenesis [65]. In

developing ARs of poplar, peu-miR160a was downregulated, while its target (*peARF17.1*) was upregulated [66]; AR formation in transgenic poplar overexpressing peu-miR160a was inhibited, whereas AR formation in polar overexpressing *PeARF17.1* or *PeARF17.2* was promoted [19]. Finally, *A. thaliana* overexpressing miR160 exhibited reduced *AtARF10* and *AtARF16* expression, shortened roots, abnormal root cap development, and uncontrolled cell division and root apical meristem (RAM) differentiation [22]. Considering the highly conserved nature of the miR160 family [67], we speculated that Ar-miR160 played an important role in AR development through the targeted cleavage of *ARF* genes.

Despite this evidence supported the important role of miR160 in AR development, the specific effects of miR160 expression tended to vary among species. For example, miR160 overexpression in poplar suppressed AR development and elongation, but overexpression of miR160a in *A. thaliana* promoted AR development [16]. Here, *A. rubrum* seedlings overexpressing Ar-miR160a generally had fewer ARs than the WT. Similar results were observed in poplar seedlings overexpressing Peu-miR160a [19].

Previous studies suggested that miR160 targeted three endogenous genes in *A. thaliana* [16]. However, none of these genes was significantly differentially expressed in transgenic *A. thaliana* overexpressing miR160 as compared to the WT, suggesting that the functions of miR160 and its target genes differed from *A. rubrum* to *A. thaliana*. Similar results were also reported in poplar [16], suggesting that in woody plants, ARF expression and AR formation might also be regulated by molecules other than miRNAs, such as long noncoding RNAs and circular RNAs [66].

Target gene function could help to clarify the miRNA function. Transgenic *A. thaliana* overexpressing *ArARF10* had more ARs than the WT; *GH3.6* expression was also significantly upregulated in the transgenic plants. *GH3* genes were highly responsive to exogenous auxin [68]; auxin then stimulated AR development by inducing the expression of the *GH3.3*, *GH3.5*, and *GH3.6* genes via the positive regulators *ARF6* and *ARF8*. Consistent with this, the three-null mutant *gh3.3gh3.5gh3.6* had fewer ARs than its wild-type counterpart [69]. These results suggested that, in *A. thaliana*, high levels of auxin led to the overexpression of *ArARF10*, stimulating AR formation. Interestingly, although *ArARF10* was functionally similar to *AtARF8* and *AtARF6*, *ArARF10* overexpression did not upregulate *GH3.3* and *GH3.5*, implying that auxin regulation pathways might differ from *A. rubrum* to *A. thaliana*. In our work, the study on Ar-miR160-*ArARF10* function in AR development of *A.rubrum* revealed the difference with that of *A. thaliana*. *AtARF17* could suppress AR development in *A. thaliana* [16], whereas *ArARF10* played a positive role in AR development in the model. Interestingly, this difference was also present between *Popolus* and *A. thaliana*. *PeARF17.1* played the similar role as *ArARF10* [19].In this study, we identified two pathways involved in the auxin response and analyzed the *ArARF* genes in those pathways. We characterized the transcription factor *ArARF10*, and separately verified the role of the Ar-miR160a-*ArARF10* interaction in AR development. We found that in AR development, Ar-miR160 acted as a negative regulator to cleave the positive regulator *ArARF10*, and the process was also integrated into the plant hormone signaling pathway and the ubiquitin mediated proteolysis pathway. Based on our results, we proposed a model clarifying the mechanisms underlying the promotion of AR growth by exogenous

auxin (**Fig. 9**): Under low auxin conditions, Aux/IAA co-inhibited ARF by recruiting TOPLESS (TPL) family and prevented the ARF activation of downstream auxin-inducible genes, regulating AR formation at the protein level [70,71]. Simultaneously, Ar-miR160 suppressed ArARF10 expression by specifically cleaving *ArARF10* mRNA, thus regulating AR formation at the transcriptional level (**Fig 9A**). When exogenous auxin levels were elevated, Aux/IAA was ubiquitinated and degraded by the SCF-type E3 ubiquitin protein ligase complex, and ARF bound to AREs in the promoters of the auxin-inducible genes to promote transcription (**Fig 9B**) [21]. The downregulation of Ar-miR160 also meant that more *ArARF10* mRNAs were translated into proteins and performed downstream functions (**Fig 9C**). In this way, *A. rubrum* responded sensitively and effectively to exogenous auxin during AR formation, leading to increased AR production. Thus, our work provided new insights into the key regulatory roles played by this module in the AR development of *A. rubrum*. ArARF10 was demonstrated to have nuclear localization and transcriptional activation.

Conclusion

In this study, the development of ARs of *A.rubrum* was significantly promoted by treatment with 300 mg/L of IBA. Changes in gene expression after exogenous auxin treatment were explored by high-throughput sequencing. We identified two key regulatory pathways (ubiquitin mediated proteolysis and plant hormone signal transduction), Ar-miR160a and the target gene *ArARF10* involved in the auxin response. Through the overexpression of *ArARF10* and Ar-miR160a, the promotion of *ArARF10* and the inhibition of Ar-miR160a on the development of ARs were found. Our results may help to study key regulatory pathways and genes for AR formation in woody plants, aiming to improve the survival rate.

Abbreviations

AR: adventitous root

miRNA: microRNA

qRT-PCR: real-time quantitative polymerase chain reaction

ARF: auxin response factors

WT: wildtype

Aux/IAA: Aux/Indole-3-Acetic Acid

TIR1: transport inhibitory response 1

AFB: AuxinBinding F-Box

LAR3: IAA-Ala Resistant3

GRF: growth-regulating factor

Seq: sequencing

CK: control

SPL: SQUAMOSA promoter-binding protein-like

ERF: ethylene response factors

IBA: Indole-3-Butytric acid

FPKM: fragments per kilobase per million

DEG: differentially expressed gene

CUL1: cullin 1

SKP1: S phase kinase-associated protein 1

MFE: minimum free energy

GFP: green fluorescent protein

GH3: gretchen hagen3

TPM: transcripts per kilobase million

MW: molecular weight

PIs: isoelectric points

NJ: Neighbor-joining

BS: bootstrap

GUS: β-glucuronidase

TPL: TOPLESS

UPS: ubiquitin–26S proteasome system

Declarations

Author Contributions

Wenpeng Zhu conducted the experiments, data analysis and wrote the manuscript. Manyu Zhang, Jianyi Li and Henwen Zhao analyzed data. Wei Ge and Kezhong Zhang designed the experiments and revised the manuscript. All authors read and approved the final draft.

Funding

This project was supported by the Beijing Excellent Training Project to WG (grant No. 68), Beijing Natural Science Fund-Municipal Education Commission Jointly Funded Projects (grant No. KZ201810020029) and Scientific Research Project of Beijing Municipal Education Commission (grant No. KM201910020005).

Acknowledgments

The authors hope to express their appreciation to the reviewers for this manuscript.

Ethics declarations

Ethics approval and consent to participate

It does not require ethical approval.

Consent for publication

Not applicable.

Competing interests

The authors declare that they have no competing interests.

References

1. Abrams, M. D. The red maple paradox. *BioScience* **48**, 355-364 (1998).
2. Lahr, E. C., Dunn, R. R. & Frank, S. D. Variation in photosynthesis and stomatal conductance among red maple (Acer rubrum) urban planted cultivars and wildtype trees in the southeastern United States. *PloS one* **13**, e0197866 (2018).
3. Pijut, P. M., Woeste, K. E. & Michler, C. H. 6 Promotion of Adventitious Root Formation of Difficult-to-Root Hardwood Tree Species. *Horticultural reviews* **38**, 213 (2011).
4. Sibley, J. L., Joseph Eakes, D., Gilliam, C. H., Keever, G. J. & Dozier Jr, W. A. Growth and fall color of red maple selections in the Southeastern United States. *Journal of Environmental Horticulture* **13**, 51-53 (1995).
5. Druege, U., Franken, P. & Hajirezaei, M. R. Plant hormone homeostasis, signaling, and function during adventitious root formation in cuttings. *Frontiers in Plant Science* **7**, 381 (2016).
6. Geiss, G., Gutierrez, L. & Bellini, C. Adventitious root formation: new insights and perspectives. *Annual plant reviews online*, 127-156 (2018).

7. Druege, U. *et al.* Molecular and physiological control of adventitious rooting in cuttings: phytohormone action meets resource allocation. *Annals of botany* **123**, 929-949 (2019).
8. Pacurar, D. I., Perrone, I. & Bellini, C. Auxin is a central player in the hormone cross-talks that control adventitious rooting. *Physiologia Plantarum* **151**, 83-96 (2014).
9. Sablowski, R. Plant stem cell niches: from signalling to execution. *Current opinion in plant biology* **14**, 4-9 (2011).
10. Guilfoyle, T. J. & Hagen, G. Auxin response factors. *Curr Opin Plant Biol* **10**, 453-460, doi:10.1016/j.pbi.2007.08.014 (2007).
11. Epstein, E. & Ludwig-Müller, J. Indole-3-butyric acid in plants: occurrence, synthesis, metabolism and transport. *Physiologia plantarum* **88**, 382-389 (1993).
12. Simon, S. & Petrášek, J. Why plants need more than one type of auxin. *Plant Science* **180**, 454-460 (2011).
13. Lakehal, A. & Bellini, C. Control of adventitious root formation: insights into synergistic and antagonistic hormonal interactions. *Physiologia plantarum* **165**, 90-100 (2019).
14. Legué, V., Rigal, A. & Bhalerao, R. P. Adventitious root formation in tree species: involvement of transcription factors. *Physiologia plantarum* **151**, 192-198 (2014).
15. Rigal, A. *et al.* The AINTEGUMENTA LIKE1 homeotic transcription factor PtAIL1 controls the formation of adventitious root primordia in poplar. *Plant Physiology* **160**, 1996-2006 (2012).
16. Gutierrez, L. *et al.* Phenotypic plasticity of adventitious rooting in Arabidopsis is controlled by complex regulation of AUXIN RESPONSE FACTOR transcripts and microRNA abundance. *The Plant Cell* **21**, 3119-3132 (2009).
17. Guilfoyle, T. J. & Hagen, G. Auxin response factors. *Current opinion in plant biology* **10**, 453-460 (2007).
18. Okushima, Y., Fukaki, H., Onoda, M., Theologis, A. & Tasaka, M. ARF7 and ARF19 regulate lateral root formation via direct activation of LBD/ASL genes in Arabidopsis. *The Plant Cell* **19**, 118-130 (2007).
19. Liu, S. *et al.* The peu-miR160a– PeARF17. 1/PeARF17. 2 module participates in the adventitious root development of poplar. *Plant biotechnology journal* **18**, 457-469 (2020).
20. Luo, J., Zhou, J.-J. & Zhang, J.-Z. Aux/IAA gene family in plants: molecular structure, regulation, and function. *International journal of molecular sciences* **19**, 259 (2018).
21. Vierstra, R. D. The ubiquitin–26S proteasome system at the nexus of plant biology. *Nature Reviews Molecular Cell Biology* **10**, 385-397 (2009).
22. Wang, J.-W. *et al.* Control of root cap formation by microRNA-targeted auxin response factors in Arabidopsis. *The Plant Cell* **17**, 2204-2216 (2005).
23. Kinoshita, N. *et al.* IAA-Ala Resistant3, an evolutionarily conserved target of miR167, mediates Arabidopsis root architecture changes during high osmotic stress. *The Plant Cell* **24**, 3590-3602 (2012).

24. Olatunji, D., Geelen, D. & Verstraeten, I. Control of endogenous auxin levels in plant root development. *International journal of molecular sciences* **18**, 2587 (2017).
25. Guo, R. *et al.* Effect of photoperiod on the formation of cherry radish root. *Scientia Horticulturae* **244**, 193-199 (2019).
26. Li, K. *et al.* miRNAs associated with auxin signaling, stress response, and cellular activities mediate adventitious root formation in apple rootstocks. *Plant Physiology and Biochemistry* **139**, 66-81 (2019).
27. Rodriguez, R. E. *et al.* MicroRNA miR396 regulates the switch between stem cells and transit-amplifying cells in Arabidopsis roots. *The Plant Cell* **27**, 3354-3366 (2015).
28. Yu, J., Liu, W., Liu, J., Qin, P. & Xu, L. Auxin control of root organogenesis from callus in tissue culture. *Frontiers in plant science* **8**, 1385 (2017).
29. Fett-Neto, A. G. *et al.* Distinct effects of auxin and light on adventitious root development in Eucalyptus saligna and Eucalyptus globulus. *Tree Physiology* **21**, 457-464 (2001).
30. Aseesh, P., Tamta, S. & Giri, D. Role of auxin on adventitious root formation and subsequent growth of cutting raised plantlets of Ginkgo biloba L. *International Journal of Biodiversity and Conservation* **3**, 142-146 (2011).
31. Guan, L. *et al.* Physiological and molecular regulation of adventitious root formation. *Critical Reviews in Plant Sciences* **34**, 506-521 (2015).
32. Weijers, D. & Wagner, D. Transcriptional responses to the auxin hormone. *Annual review of plant biology* **67**, 539-574 (2016).
33. Agulló-Antón, M. Á., Sánchez-Bravo, J., Acosta, M. & Druege, U. Auxins or sugars: what makes the difference in the adventitious rooting of stored carnation cuttings? *Journal of Plant Growth Regulation* **30**, 100-113 (2011).
34. Agulló-Antón, M. Á. *et al.* Early steps of adventitious rooting: morphology, hormonal profiling and carbohydrate turnover in carnation stem cuttings. *Physiologia plantarum* **150**, 446-462 (2014).
35. Villacorta-Martín, C. *et al.* Gene expression profiling during adventitious root formation in carnation stem cuttings. *BMC genomics* **16**, 1-18 (2015).
36. Kelley, D. R. & Estelle, M. Ubiquitin-mediated control of plant hormone signaling. *Plant physiology* **160**, 47-55 (2012).
37. Calderon-Villalobos, L. I., Tan, X., Zheng, N. & Estelle, M. Auxin perception—structural insights. *Cold Spring Harbor perspectives in biology* **2**, a005546 (2010).
38. Vierstra, R. D. The ubiquitin/26S proteasome pathway, the complex last chapter in the life of many plant proteins. *Trends in plant science* **8**, 135-142 (2003).
39. Salehin, M., Bagchi, R. & Estelle, M. SCFTIR1/AFB-based auxin perception: mechanism and role in plant growth and development. *The Plant Cell* **27**, 9-19 (2015).
40. Villalobos, L. I. A. C. *et al.* A combinatorial TIR1/AFB–Aux/IAA co-receptor system for differential sensing of auxin. *Nature chemical biology* **8**, 477-485 (2012).

41. Tan, X. *et al.* Mechanism of auxin perception by the TIR1 ubiquitin ligase. *Nature* **446**, 640-645 (2007).
42. Walsh, T. A. *et al.* Mutations in an auxin receptor homolog AFB5 and in SGT1b confer resistance to synthetic picolinate auxins and not to 2, 4-dichlorophenoxyacetic acid or indole-3-acetic acid in Arabidopsis. *Plant physiology* **142**, 542-552 (2006).
43. Dreher, K. A., Brown, J., Saw, R. E. & Callis, J. The Arabidopsis Aux/IAA protein family has diversified in degradation and auxin responsiveness. *The Plant Cell* **18**, 699-714 (2006).
44. Tiwari, S. B., Hagen, G. & Guilfoyle, T. J. Aux/IAA proteins contain a potent transcriptional repression domain. *The Plant Cell* **16**, 533-543 (2004).
45. Weijers, D. *et al.* Developmental specificity of auxin response by pairs of ARF and Aux/IAA transcriptional regulators. *The EMBO journal* **24**, 1874-1885 (2005).
46. Parry, G. *et al.* Complex regulation of the TIR1/AFB family of auxin receptors. *Proceedings of the National Academy of Sciences* **106**, 22540-22545 (2009).
47. Roosjen, M., Paque, S. & Weijers, D. Auxin response factors: output control in auxin biology. *Journal of experimental botany* **69**, 179-188 (2018).
48. Nanao, M. H. *et al.* Structural basis for oligomerization of auxin transcriptional regulators. *Nature communications* **5**, 1-8 (2014).
49. Peng, Y., Fang, T., Zhang, Y., Zhang, M. & Zeng, L. Genome-Wide Identification and Expression Analysis of Auxin Response Factor (ARF) Gene Family in Longan (Dimocarpus longan L.). *Plants* **9**, 221 (2020).
50. Li, S.-B. *et al.* Genome-wide identification, isolation and expression analysis of auxin response factor (ARF) gene family in sweet orange (Citrus sinensis). *Frontiers in Plant Science* **6**, 119 (2015).
51. Piya, S., Shrestha, S. K., Binder, B., Stewart Jr, C. N. & Hewezi, T. Protein-protein interaction and gene co-expression maps of ARFs and Aux/IAAs in Arabidopsis. *Frontiers in plant science* **5**, 744 (2014).
52. Finet, C., Berne-Dedieu, A., Scutt, C. P. & Marlétaz, F. Evolution of the ARF gene family in land plants: old domains, new tricks. *Molecular Biology and Evolution* **30**, 45-56 (2013).
53. Li, S.-B., Xie, Z.-Z., Hu, C.-G. & Zhang, J.-Z. A review of auxin response factors (ARFs) in plants. *Frontiers in plant science* **7**, 47 (2016).
54. Bailey, T. L. *et al.* MEME SUITE: tools for motif discovery and searching. *Nucleic acids research* **37**, W202-W208 (2009).
55. Xie, R. *et al.* The ARF, AUX/IAA and GH3 gene families in citrus: genome-wide identification and expression analysis during fruitlet drop from abscission zone A. *Molecular Genetics and Genomics* **290**, 2089-2105 (2015).
56. Jiao, Y. *et al.* Ancestral polyploidy in seed plants and angiosperms. *Nature* **473**, 97-100 (2011).
57. Overvoorde, P., Fukaki, H. & Beeckman, T. Auxin control of root development. *Cold Spring Harbor perspectives in biology* **2**, a001537 (2010).

58. Ha, M. & Kim, V. N. Regulation of microRNA biogenesis. *Nature reviews Molecular cell biology* **15**, 509-524 (2014).
59. Llave, C., Xie, Z., Kasschau, K. D. & Carrington, J. C. Cleavage of Scarecrow-like mRNA targets directed by a class of Arabidopsis miRNA. *Science* **297**, 2053-2056 (2002).
60. Song, L., Axtell, M. J. & Fedoroff, N. V. RNA secondary structural determinants of miRNA precursor processing in Arabidopsis. *Current Biology* **20**, 37-41 (2010).
61. Wang, L., Mai, Y.-X., Zhang, Y.-C., Luo, Q. & Yang, H.-Q. MicroRNA171c-targeted SCL6-II, SCL6-III, and SCL6-IV genes regulate shoot branching in Arabidopsis. *Molecular plant* **3**, 794-806 (2010).
62. Yu, N., Niu, Q. W., Ng, K. H. & Chua, N. H. The role of miR156/SPL s modules in Arabidopsis lateral root development. *The Plant Journal* **83**, 673-685 (2015).
63. Xu, X. *et al.* High miR156 expression is required for auxin-induced adventitious root formation via MxSPL26 independent of PINs and ARFs in Malus xiaojinensis. *Frontiers in plant science* **8**, 1059 (2017).
64. Bustos-Sanmamed, P. *et al.* Overexpression of miR160 affects root growth and nitrogen-fixing nodule number in Medicago truncatula. *Functional Plant Biology* **40**, 1208-1220 (2013).
65. Lin, Y. *et al.* Endogenous target mimics down-regulate miR160 mediation of ARF10,-16, and-17 cleavage during somatic embryogenesis in Dimocarpus longan Lour. *Frontiers in plant science* **6**, 956 (2015).
66. Liu, S., Wu, L., Qi, H. & Xu, M. LncRNA/circRNA–miRNA–mRNA networks regulate the development of root and shoot meristems of Populus. *Industrial Crops and Products* **133**, 333-347 (2019).
67. Zhang, B., Pan, X., Cobb, G. P. & Anderson, T. A. Plant microRNA: a small regulatory molecule with big impact. *Developmental biology* **289**, 3-16 (2006).
68. Park, J.-E. *et al.* GH3-mediated auxin homeostasis links growth regulation with stress adaptation response in Arabidopsis. *Journal of Biological Chemistry* **282**, 10036-10046 (2007).
69. Gutierrez, L. *et al.* Auxin controls Arabidopsis adventitious root initiation by regulating jasmonic acid homeostasis. *The Plant Cell* **24**, 2515-2527 (2012).
70. Leyser, O. Auxin signaling. *Plant physiology* **176**, 465-479 (2018).
71. Iwakawa, H.-o. & Tomari, Y. The functions of microRNAs: mRNA decay and translational repression. *Trends in cell biology* **25**, 651-665 (2015).
72. Grabherr, M. G. *et al.* Full-length transcriptome assembly from RNA-Seq data without a reference genome. *Nature biotechnology* **29**, 644-652 (2011).
73. Pertea, G. *et al.* TIGR Gene Indices clustering tools (TGICL): a software system for fast clustering of large EST datasets. *Bioinformatics* **19**, 651-652 (2003).
74. Simão, F. A., Waterhouse, R. M., Ioannidis, P., Kriventseva, E. V. & Zdobnov, E. M. BUSCO: assessing genome assembly and annotation completeness with single-copy orthologs. *Bioinformatics* **31**, 3210-3212 (2015).

75. Trapnell, C. *et al.* Differential gene and transcript expression analysis of RNA-seq experiments with TopHat and Cufflinks. *Nature protocols* **7**, 562-578 (2012).
76. Wang, L., Feng, Z., Wang, X., Wang, X. & Zhang, X. DEGseq: an R package for identifying differentially expressed genes from RNA-seq data. *Bioinformatics* **26**, 136-138 (2010).
77. Evers, M., Huttner, M., Dueck, A., Meister, G. & Engelmann, J. C. miRA: adaptable novel miRNA identification in plants using small RNA sequencing data. *BMC bioinformatics* **16**, 1-10 (2015).
78. 't Hoen, P. A. *et al.* Deep sequencing-based expression analysis shows major advances in robustness, resolution and inter-lab portability over five microarray platforms. *Nucleic acids research* **36**, e141-e141 (2008).
79. Anders, S. & Huber, W. Differential expression analysis for sequence count data. *Nature Precedings*, 1-1 (2010).
80. Bo, X. & Wang, S. TargetFinder: a software for antisense oligonucleotide target site selection based on MAST and secondary structures of target mRNA. *Bioinformatics* **21**, 1401-1402 (2005).
81. Addo-Quaye, C., Miller, W. & Axtell, M. J. CleaveLand: a pipeline for using degradome data to find cleaved small RNA targets. *Bioinformatics* **25**, 130-131 (2009).
82. Meyers, B. C. *et al.* Criteria for annotation of plant MicroRNAs. *The Plant Cell* **20**, 3186-3190 (2008).
83. Zuker, M. & Stiegler, P. Optimal computer folding of large RNA sequences using thermodynamics and auxiliary information. *Nucleic acids research* **9**, 133-148 (1981).
84. Chen, C. *et al.* TBtools: an integrative toolkit developed for interactive analyses of big biological data. *Molecular plant* **13**, 1194-1202 (2020).
85. Peng, Y., Fang, T., Zhang, Y., Zhang, M. & Zeng, L. Genome-Wide Identification and Expression Analysis of Auxin Response Factor (ARF) Gene Family in Longan (Dimocarpus longan L.). *Plants (Basel)* **9**, doi:10.3390/plants9020221 (2020).
86. Li, S. B. *et al.* Genome-wide identification, isolation and expression analysis of auxin response factor (ARF) gene family in sweet orange (Citrus sinensis). *Front Plant Sci* **6**, 119, doi:10.3389/fpls.2015.00119 (2015).
87. El-Gebali, S. *et al.* The Pfam protein families database in 2019. *Nucleic acids research* **47**, D427-D432 (2019).
88. Kumar, S., Stecher, G. & Tamura, K. MEGA7: molecular evolutionary genetics analysis version 7.0 for bigger datasets. *Molecular biology and evolution* **33**, 1870-1874 (2016).
89. Nei, M. & Kumar, S. *Molecular evolution and phylogenetics*. (Oxford university press, 2000).
90. Bailey, T. L. & Elkan, C. in *Ismb.* 21-29.
91. Chen, C. *et al.* TBtools-an integrative toolkit developed for interactive analyses of big biological data. *bioRxiv*, 289660 (2020).
92. Lin, Y. L. & Lai, Z. X. Evaluation of suitable reference genes for normalization of microRNA expression by real-time reverse transcription PCR analysis during longan somatic embryogenesis. *Plant physiology and biochemistry* **66**, 20-25 (2013).

93. Zhu, L. *et al.* Reference Gene Selection for Quantitative Real-Time PCR Analyses of Acer palmatum under Abiotic Stress. *Phyton* **89**, 385 (2020).
94. Livak, K. J. & Schmittgen, T. D. Analysis of relative gene expression data using real-time quantitative PCR and the 2− ΔΔCT method. *methods* **25**, 402-408 (2001).
95. Lichocka, M. & Schmelzer, E. Subcellular localization experiments and FRET-FLIM measurements in plants. *Bio-protocol* **4**, 1-12 (2014).
96. Sorin, C. *et al.* Auxin and light control of adventitious rooting in Arabidopsis require ARGONAUTE1. *The Plant Cell* **17**, 1343-1359 (2005).
97. Collins, T. J. ImageJ for microscopy. *Biotechniques* **43**, S25-S30 (2007).

Figures

Figure 1

AR formation in A. rubrum cuttings treated with 100–500 mg/L IBA and untreated water (CK). With the increase of IBA concentration, the number of ARs showed a trend of increasing and then decreasing and reached a peak at IBA 300 mg/L.

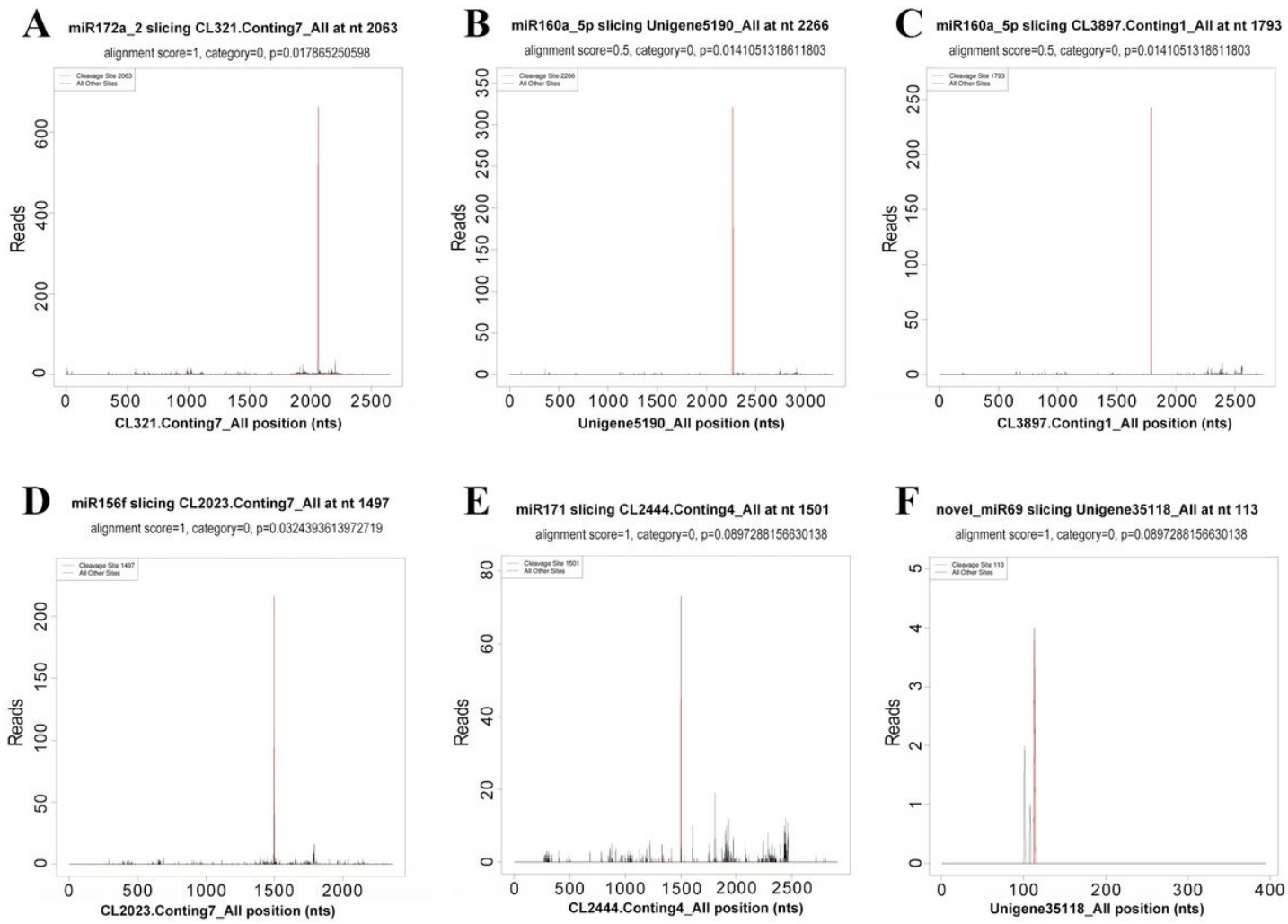

Figure 2

Identification of candidate miRNA targets using degradome sequencing. Six targets of five conserved and one novel miRNAs were shown in the panels as example. The x-axis indicated the position of target genes while the y-axis represented the abundance of sequenced reads. Each line was a degradome fragment that could be mapped to the corresponding target gene and the red line indicated the expected miRNA positions. Category0: where the original data fragment was located, the abundance was equal to the maximum abundance on the mRNA, and there was only one maximum.

Figure 3

Hierarchical clustering of the differentially expressed genes associated with the major regulatory pathways. Bars represented scales of pathway expression levels (log 2), from up-regulated (red) to down-regulated (blue).

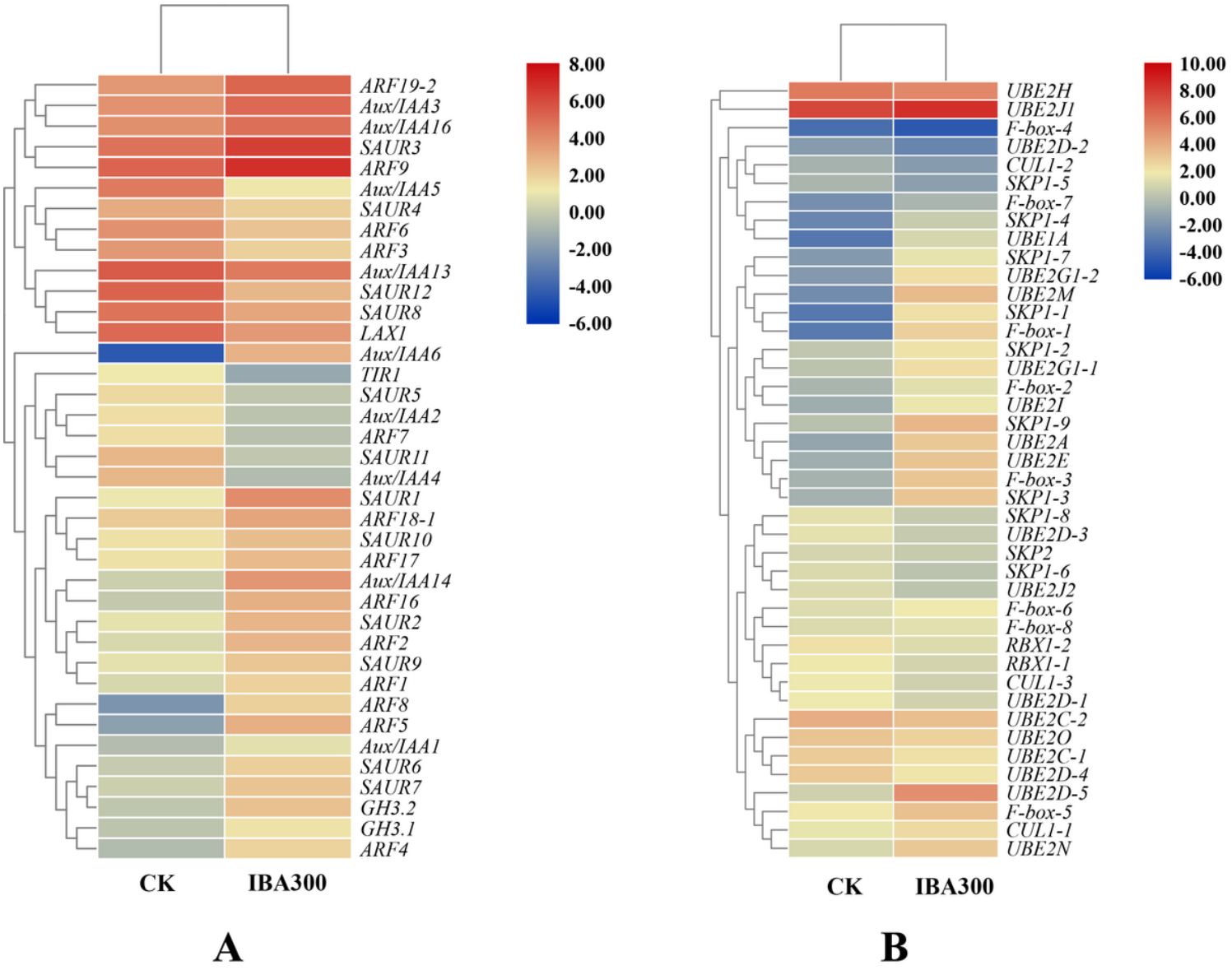

Figure 4

Hierarchical clustering of the differentially expressed genes in the key pathways. (A) Plant hormone signaling pathway. (B) Ubiquitin mediated proteolysis pathway.

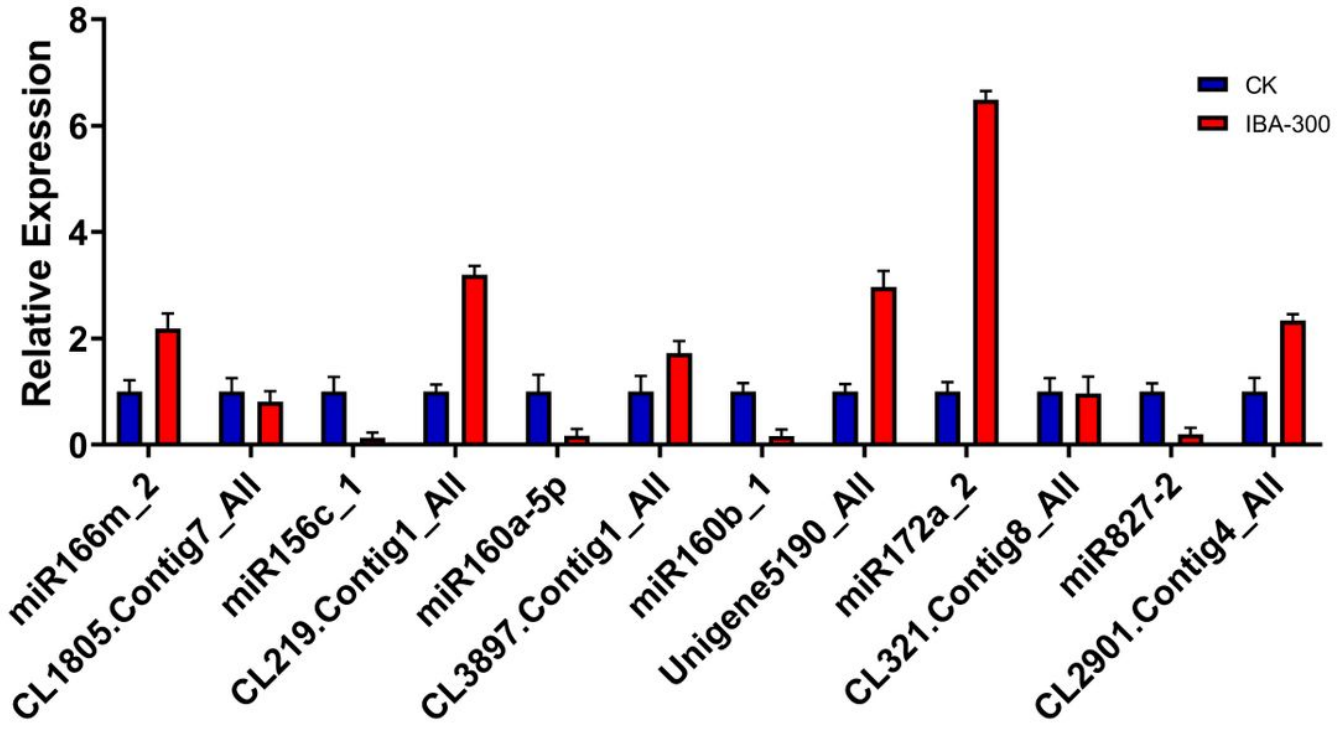

Figure 5

Relative expression levels of six miRNAs and target genes. Actin6 was used as a reference for mRNA qRT-PCR while U6 snRNA was used for the miRNA qRT-PCR. The expression in the control was set to 1.0. Mean values of three replicates were shown with standard error bars.

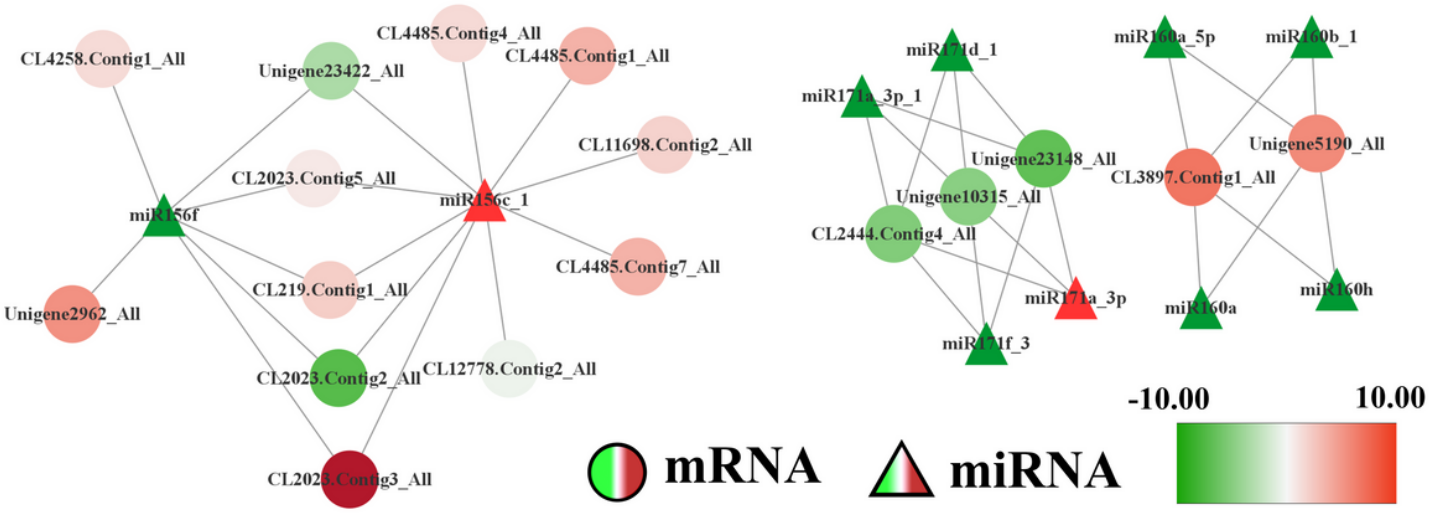

Figure 6

The miRNA-mRNA regulation networks of Ar-miR160a-5p, Ar-miR171d-1 and Ar-miR156f. Upregulated genes/miRNAs were shown in red; downregulated genes/miRNAs were shown in green.

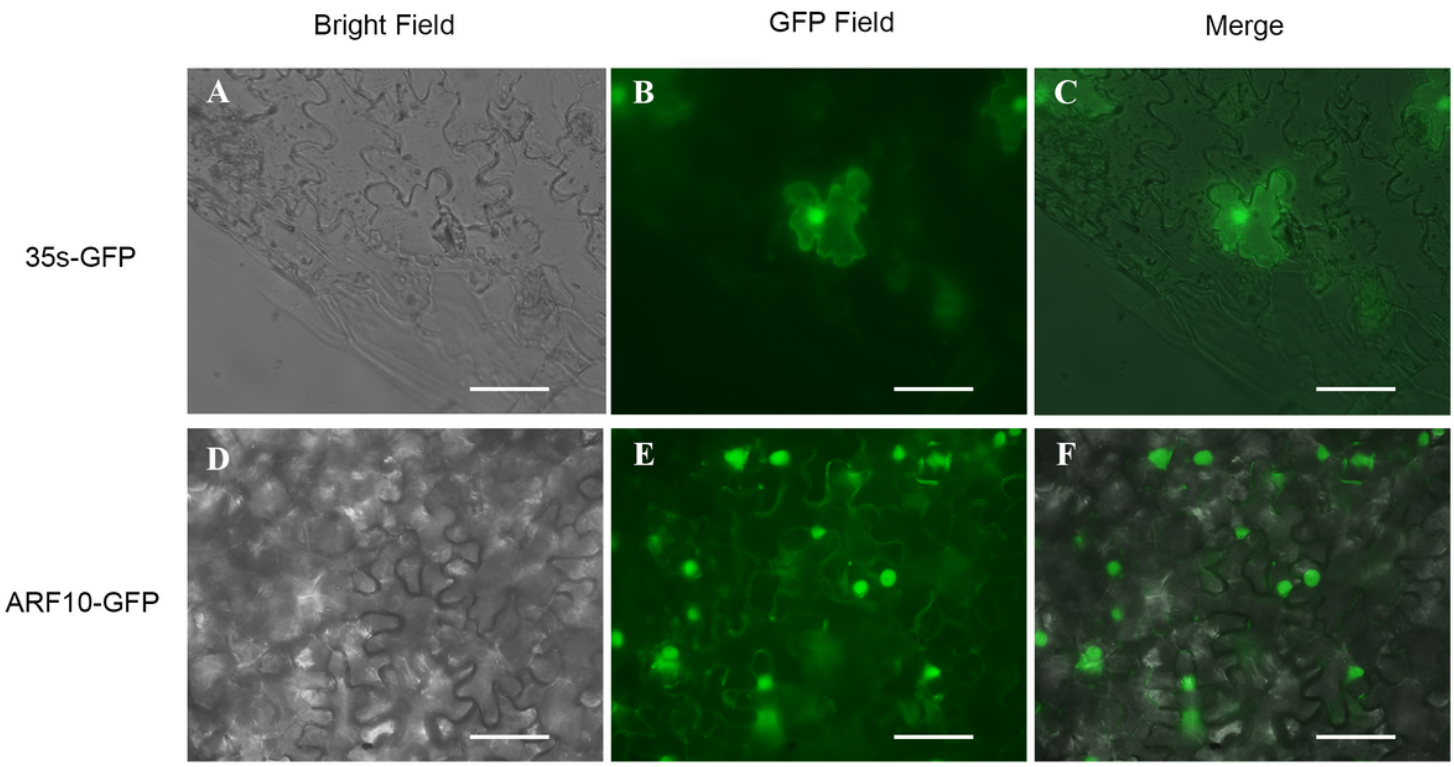

Figure 7

Subcellular localization of ArARF10. (A-C) N. benthamiana cells expressing 35S-GFP. (D–F) N. benthamiana cells expressing ArARF10-GFP. Bar = 50μm.

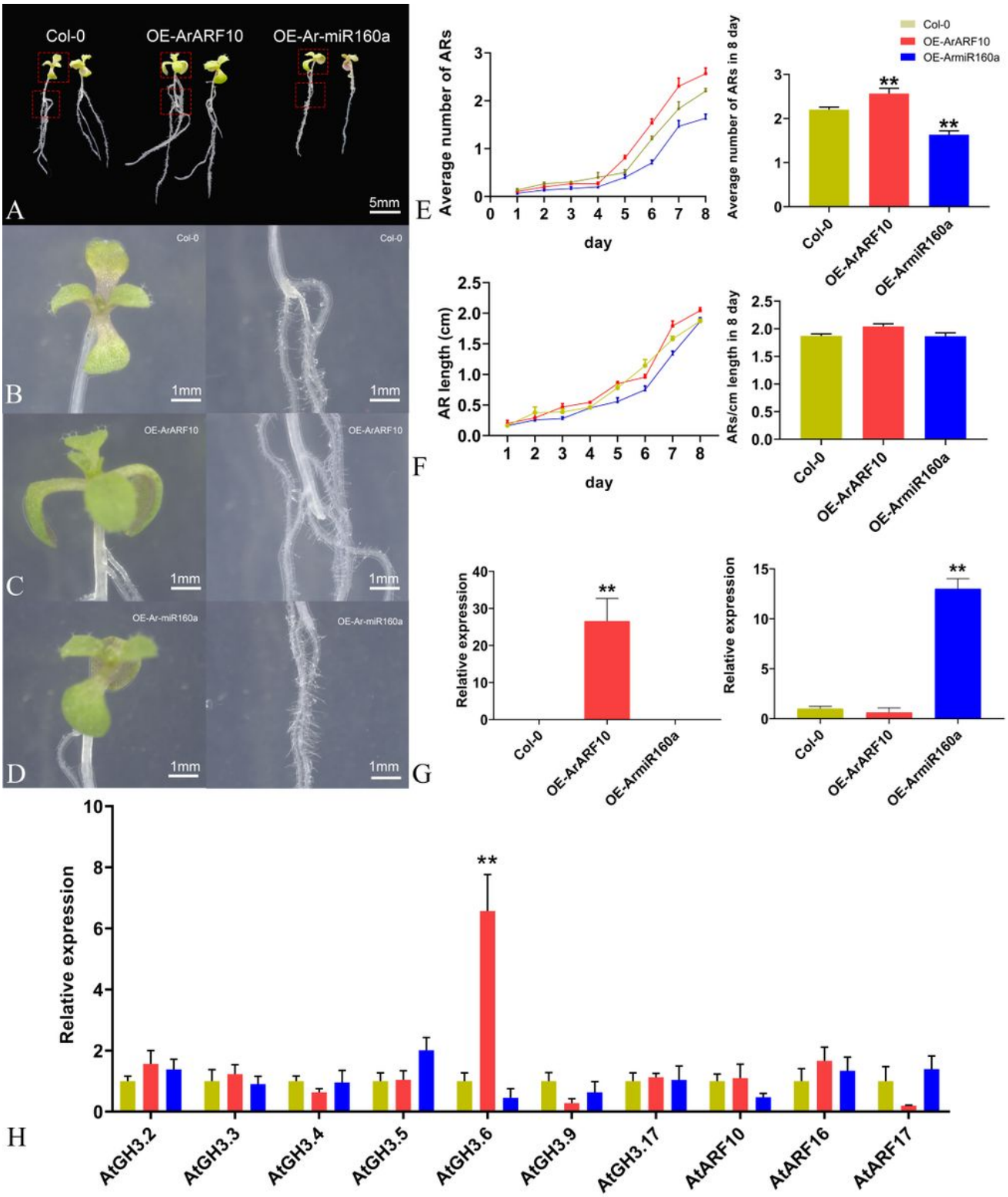

Figure 8

AR formation in transgenic A.thaliana overexpressing ArARF10 and Ar-miR160a. (A) Comparison of OE-ArARF10 and OE-Ar-miR160a transgenic plant with Col-0 types. Bar = 5mm. (B) ARs in WT phenotypes under long daylight incubation for eight days. (C) Overexpression of ArARF10 promoted the AR formation. (D) Overexpression of Ar-miR160a inhibited the AR formation. Bar = 1 mm.(E) Left panel showed changes in the number of ARs in Col-0, OE-ArARF10 and OE-Ar-miR160a transgenic lines over 8 days. Right panel

showed the number recorded on day 8, with a significant increase in OE-ArARF10 ARs and a significant decrease in OE-Ar-miR160a ARs compared to WT. Error bars indicated the mean SE (**p<0.01, n=3). (F) Left panel showed the changes in AR length in Col-0 and OE-ArARF10 and OE-Ar-miR160a transgenic lines over 8 days. Right panel showed the AR length recorded on day 8, with few change in the AR length of OE-ArARF10 and OE-Ar-miR160a compared to WT. (G)The relative expression levels of ArARF10 in OE-ArARF10 (left panel) and Ar-miR160a in OE-Ar-miR160a (right panel). (H) Expression patterns of endogenous genes in transgenic plants and Col-0 types. The error bars indicate the mean SE (**p<0.01, n=3).

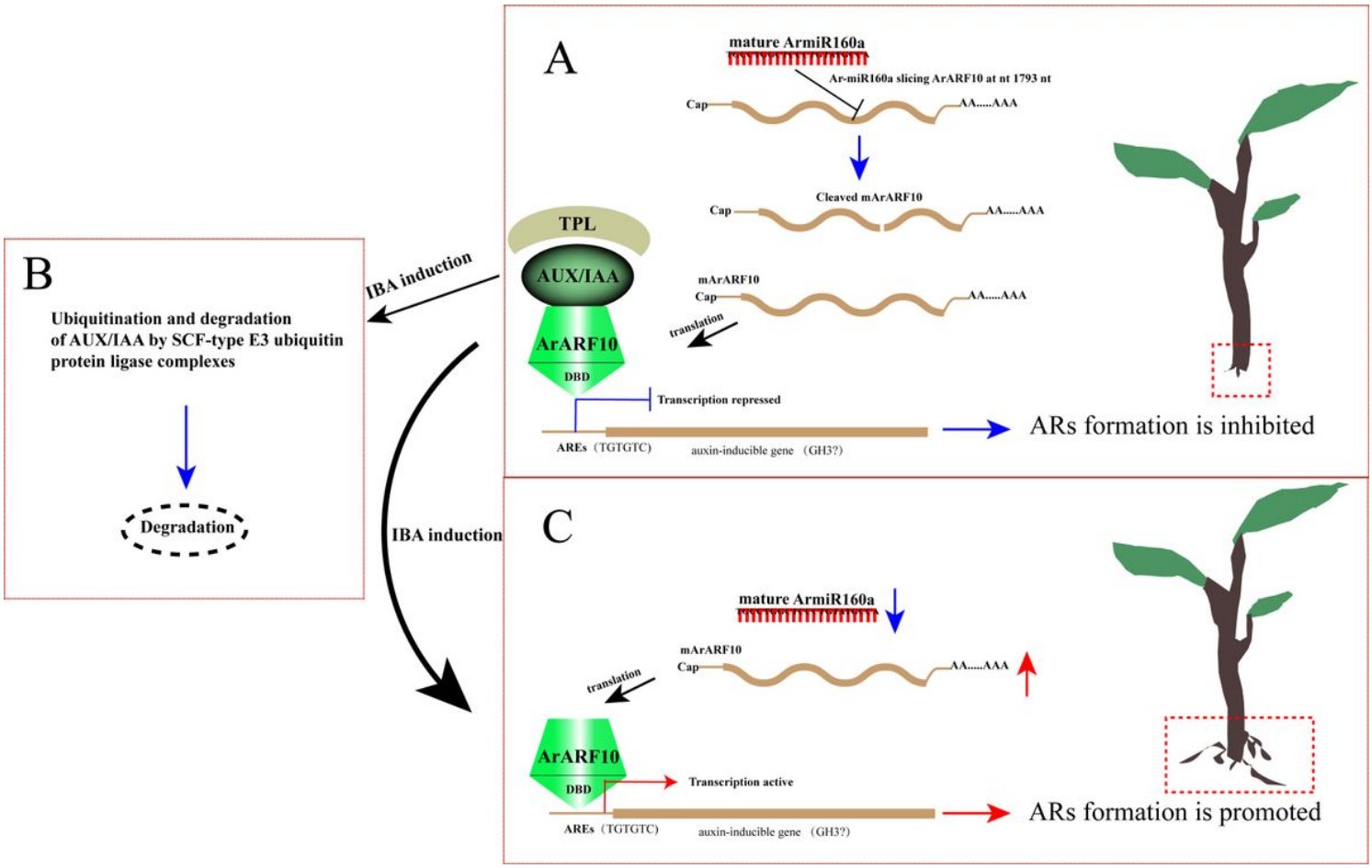

Figure 9

Schematic presentation of regulatory events of AR growth in A. rubrum. (A) Under low auxin conditions, Ar-miR160 specifically cleaved mRNA-ArARF10 to repress ArARF10 expression, while Aux/IAA prevented Auxin-inducible gene transcription by recruiting TPL to co-inhibit ArARF10 binding to AREs in the Auxin-inducible gene promoter. (B) When exogenous auxin levels were increased, Aux/IAA was ubiquitinated and degraded by the SCF-type E3 ubiquitin protein ligase complex, and ArARF10 bound to AREs in the promoter of auxin-inducible genes to promote transcription. (C) The reduced expression of Ar-miR160 also meant that more mRNA-ArARF10 was translated into protein and performed downstream functions that promoted the AR formation.

Supplementary Files

This is a list of supplementary files associated with this preprint. Click to download.

- Supplementaryfile.docx